

Soft Matter

Accepted Manuscript



This is an *Accepted Manuscript*, which has been through the Royal Society of Chemistry peer review process and has been accepted for publication.

Accepted Manuscripts are published online shortly after acceptance, before technical editing, formatting and proof reading. Using this free service, authors can make their results available to the community, in citable form, before we publish the edited article. We will replace this *Accepted Manuscript* with the edited and formatted *Advance Article* as soon as it is available.

You can find more information about *Accepted Manuscripts* in the [Information for Authors](#).

Please note that technical editing may introduce minor changes to the text and/or graphics, which may alter content. The journal's standard [Terms & Conditions](#) and the [Ethical guidelines](#) still apply. In no event shall the Royal Society of Chemistry be held responsible for any errors or omissions in this *Accepted Manuscript* or any consequences arising from the use of any information it contains.

Cite this: DOI: 10.1039/c0xx00000x

www.rsc.org/xxxxxx

ARTICLE TYPE**Analysis of linear viscoelastic behaviour of alginate gel: effects of inner relaxation, water diffusion, and syneresis**Ciro Siviello,^a Francesco Greco^b and Domenico Larobina^{*a}

Received (in XXX, XXX) Xth XXXXXXXXX 20XX, Accepted Xth XXXXXXXXX 20XX

DOI: 10.1039/b000000x

The mechanical behaviour of ionically cross-linked alginate gels is here investigated in detail. To determine the range of linear response of the material, experiments of uniaxial unconfined compression and torsional deformation are performed, obtaining both the stress-strain and the viscoelastic behaviour of the gel. On-line measurements of the radius of the cylindrical gel sample in those experiments are also reported. The linearity range in the gel mechanical response is found to be rather limited, up to 6% strain, at most, contrary to more optimistic conclusions usually reported in the literature. We confirm the presence of a stress-diffusion coupling phenomenon in our alginates, i.e., the migration of water from/into the gel in response to the applied deformation. A phenomenon of inner (constitutive) relaxation of the network component of the gel is also clearly identified, and observed to occur, in parallel with solvent diffusion, upon compression. At sufficiently large times after a step deformation, syneresis is always found, with concomitant nonstandard viscoelastic effects such as the growth of a normal force in torsion, and a size dependent decay of the longitudinal force in compression. We applied a *two-fluid model*, recently developed by two of the present authors [Larobina, D., & Greco, F. (2012). *The Journal of Chemical Physics*, 136(13), 134904], to simulate the relaxation tests upon torsional and compressive deformations, and to fit our own experiments. The model is found to well describe the coupling between constitutive relaxation and diffusion, and to reproduce the available forces and radii data before the advent of syneresis.

Introduction

Gels are soft materials made by a three-dimensional network swollen by a liquid component. The swollen network confers the characteristic solid-like properties to the gel, while the liquid controls its density. The network can be formed by physical or chemical ‘junctions’. In the former case we talk of physical gels, and the junctions are characterized by a finite (although sometimes large) lifetime. In the latter case, instead, we have a chemical gel, and its junctions are permanent covalent bonds (cross-links). Consequently, physical gels can display viscoelastic response as results of inner relaxation,^{1,2} while covalent gels are often considered to be elastic materials.^{3,4}

Although the liquid phase occupies majority of gel volume, the gel does not display any flow at rest. When the gel, at equilibrium with its liquid, is compressed (elongated), the liquid will slowly diffuse out (in) of the gel, causing a relaxation of the applied force.^{5,6} It should however be mentioned that such stress-induced liquid diffusion is not the only mechanism of fluid motions inside the gel. Indeed, spontaneous expulsion of liquid after a certain time span is frequently encountered in physical gels. The phenomenon is known as syneresis, and takes place mainly as

results of *slow* rearrangements of the network.^{7,8}

In this contribution, we decide to focus our attention on the mechanical behaviour of ionically cross-linked alginate gels. The reasons are manifold: first, alginates are of strong interest in food industry⁹, biology¹⁰, and tissue engineering¹¹; moreover, they are easy to prepare; and, last, they can be taken as valid models of the whole class of ionic gels.

Alginates are polysaccharides extracted from brown algae and bacteria.¹² They are random block co-polymers containing β -(14)-linked D-mannuronic acid (M) and α -(14)-linked L-guluronic acid (G) residues. In order to form a gel, alginates need to come into contact with divalent ions (such as Ca^{2+} , Ba^{2+} , Sr^{2+} , just to mention a few). Actually, almost all divalent ions are able to form specific multiple complex junctions with G-blocks units; such junctions, sometime termed ‘egg-boxes’,¹³ are responsible for the distinctive mechanical response of alginate hydrogels, including their viscoelastic relaxation, and fracture toughness.¹⁴

The prevailing literature has depicted alginate gels as elastic materials, with compression moduli ranging from a *kPa* to a hundred of *kPa*.^{12,15} The linear elastic behaviour is thought to be quite extended. Indeed, by examining the stress-strain behaviour of alginate hydrogels, Mooney and co workers¹ claimed that linearity extends up to 15% of compression. At higher

compressions, other authors¹⁵ have observed an upward concavity in the stress-strain curve.

Viscoelastic properties of alginate were also investigated by several authors using frequency sweep tests,¹⁶⁻¹⁸ and relaxation tests upon torsion or compression.^{1,19-24} Among them, Webber and Shull (2004) studied the dependency of the physical network response on the amplitude of the strain, by using an indentation apparatus. They showed that at small strains the alginate gels behave elastically, with little non-recoverable creep and with dynamic moduli that are only weakly frequency dependent; at higher strain magnitudes, instead, the gels have a viscoelastic behaviour.

In this paper, in order to fully ascertain the range of mechanical linear response of the gel, we decided to perform three distinct sets of experiments. First, an uniaxial unconfined compression test is made, to obtain the stress-strain behaviour of the sample. Second, stress evolution of the uniaxially strained gel is followed in time, upon different imposed compressions, to investigate on the relaxation behaviour of the sample. Finally, the gel response for a different strain configuration, namely, under torsional deformations, is measured, both after a step torsion ('instantaneous' elasticity and ensuing relaxation) and under a small-amplitude oscillating strain, so as to possibly confirm the full linearity range identified in the two previous sets of experiments. Alongside with all those stress-strain experiments, a 'geometric' characterization of the sample is always given, by on-line measurements of the radius of the cylindrical specimens at hand. Moreover, most of the above-indicated experiments were performed for three different (initial) radii of the cylindrical sample, so as to detect possible size effects on the rheological response of our gel. Indeed, through these observations, we aim to quantify stress-diffusion coupling, if any, i.e., the possible migration of water from/into the gel in response to the applied deformation.

Material and Methods

Gel preparation

Calcium alginate gel samples were prepared using a two-step procedure. The first step involves the manufacture of a gel with well-defined and stable shape by 'inner gelation' mechanism. In the second step, instead, we expose the pre-shaped gel to a calcium chloride solution of known concentration for a certain amount of time at constant temperature. Details of the 'inner gelation' mechanism can be found on reference.²⁵ Briefly, a 2%w/w alginate solution is mixed with an insoluble calcium complex form (calcium ethylene-diamine-tetraacetic, CaEDTA) to a final concentration of 5 mM CaEDTA. The stable solution is then additivated with an hydrolysable lactone (Glucono-d-lactone, GDL) and immediately casted into a cylindrical preform. The addition of GDL slowly decreases the pH of the solution inducing the release of calcium ion from the insoluble CaEDTA salt, and producing a gel with stable cylindrical shape. All pre-formed gels had a diameter of 35 mm and a thickness of 7 mm. In the second step, the cylindrical pre-formed gels were simply immersed into a 5 mM solution of CaCl₂ for 24 hours at 25°C.

Mechanical tests

Mechanical testing of alginate samples were carried out with a

HAAKE MARS III rheometer coupled with a CCD camera to quantify the lateral radius of the sample during tests. All experiments were performed at 25°C using a plate-plate geometry. Depending on the type of test, a compressive or a torsional force is applied on the sample. The performed compression tests were: i) stress-strain measurements on samples of 15 mm diameter at different strain-rate; ii) stress-relaxation measurements on samples of 15 mm diameter at different strains; iii) stress-relaxation measurements at 3% of strain on samples with different diameters, i.e. 15, 24 and 35 mm. To ensure a slip condition at wall during compression a vaseline layer was placed on both plates.

The executed torsional tests, instead, were: i) oscillatory amplitude sweep on sample of 35 mm diameter at 1 Hz; ii) oscillatory frequency sweep with samples of 35 mm diameter at 1% of amplitude strain; iii) stress-relaxation measurements at 3% of strain, again on samples with different diameters, i.e. 15, 24 and 35 mm. Opposite to compressive test, a cyanoacrylate glue was placed between the plates and the gel surfaces, so to avoid slip of the specimen during torsion.

To prevent solvent evaporation during test, a CaCl₂ solution at 5 mM was always surrounding the samples. Moreover, in the case of tests with samples of 15 and 24 mm diameter, the specimens were cut from the 24 hours conditioned samples of 35 mm right before testing. This procedure guarantees that all specimens had experienced the same conditions regardless of the size of the sample tested.

It is worth to point out that the characteristic time of applied deformation is different for the different geometric test configurations. Specifically, for torsional experiments the time of application of the strain is about 10⁻² min (0.6 s), while, for compressional tests it is only 10⁻¹ min (6s).

Results and Discussion

'Instantaneous' elasticity

Stress-strain compressive tests at different strain rates were performed, measuring compressive force f and radius r of the cylindrical sample as function of applied longitudinal stretch ratio $\lambda \equiv h(t)/h_0$, where $h(t)$ is the height of the specimens as function of time, and h_0 its initial value. The rate of strain was varied in the range 0.06 to 2 min⁻¹, and a cumulative strain down to $\lambda = 0.77$ was reached, i.e., with ca. 25% compression of the sample. Within the experimental error, neither the force nor the radius showed any noticeable dependence on the imposed strain rate. Hence, both $f(\lambda)$ and $r(\lambda)$ can be unambiguously defined within the indicated ranges of strain and strain rates (and before any relaxation occur, see the next subsection); because of the absence of time effects, we refer to our results in this subsection as pertaining to an 'instantaneous' elasticity of the gel.

Let us discuss the 'geometric' (lateral expansion) aspects of our compression tests first. We report, in Fig.1, the measured 'transverse ratio' $\lambda_T \equiv r(\lambda)/R_0$ as a function of the longitudinal ratio λ , along with the theoretical prediction $\lambda_{T,incorp} = \lambda^{-0.5}$ (continuous line) calculated through the assumption of incompressibility. As it can be seen, the lateral dilation of the cylindrical specimen almost exactly follows the theoretical curve for small deformations (down to $\lambda \approx 0.94$, say), to progressively

depart from the theory at lower λ -values.

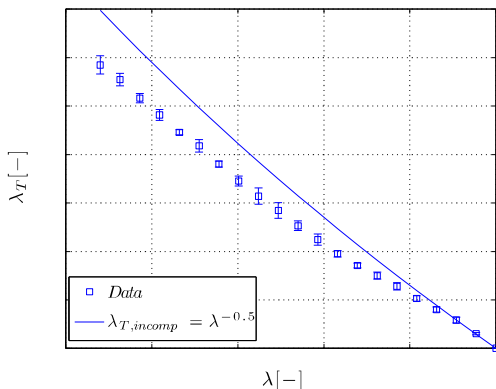


Figure 1. Transverse dilation ratio (λ_T) as function of the compressive ratio (λ) for samples compressed at different strain rates (ranging from 0.06 to 2 min^{-1}). Symbols are data averaged over twenty runs, while continuous line is the prediction assuming incompressibility.

As a numerical example, at a longitudinal ratio $\lambda = 0.816$, we measure $\lambda_T = 1.089$, whereas it is $\lambda_{T,incomp} = 1.107$: the radius of the sample turns out to be ca. 2% lower than its predicted value for a perfectly incompressible gel. The observed discrepancy between λ_T and $\lambda_{T,incomp}$ below $\lambda = 0.94$ is confirmed, in trend, by an independent measurement of mass loss from the gel as a function of the compressive ratio.

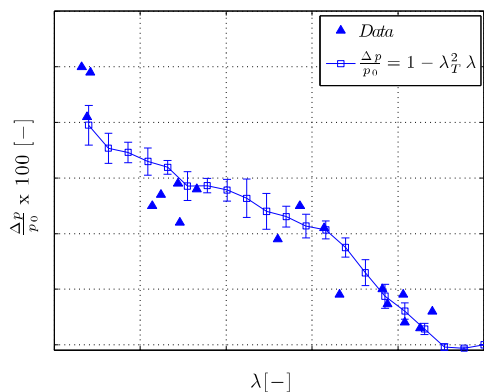


Figure 2. Relative weight loss at the end of compression as function of final compressive ratio. Full symbols are data, while open symbols are calculated (through eq. 1) from the measured transverse dilation ratio (see Fig. 1), assuming that the two media (water and alginate) are incompressible and with equal densities ($\rho_{H_2O} = \rho_{polymer} = 1 \text{ g/cm}^3$). The line through the calculated points is just a guide for the eye.

Specifically, the cylindrical specimen at the end of a compression ramp was extracted from the apparatus and weighed, for several values of the final compressive ratio: the measured relative weight loss $\Delta p/p_0$ as a function of the attained compression is reported in Fig.2 (filled symbols). On the other hand, from the knowledge of the actual lateral dilation as function of the compressive ratio, $\lambda_T(\lambda)$ (see Fig.1), it is possible to estimate the mass loss during compression. Indeed, by assuming an equal density of the two media (water and alginate) composing the gel, and a nil volume change on mixing (ideal mixing), the relative weight loss is easily calculated as:

$$\frac{\Delta p}{p_0} = 1 - \lambda_T^2 \lambda \quad (1)$$

The mass loss from Eq.1 is also reported in figure 2 (open symbols).

Notwithstanding the scattering of data, the trend in Fig.2 is clear: unless very low compressions are considered, the higher is the final compression the higher is the mass loss. Such behaviour is seen to be coherent, at least, with that of the transverse ratio λ_T , which increases with the imposed compression less than the $\lambda_{T,incomp}$ pertaining to an ideally incompressible material (Fig.1). We are inclined to attribute those compression-induced phenomena, i.e. the weight loss and the non-ideality in the change of the transverse ratio, to an escape of water from the alginate network by some kind of convective mechanism. This mechanism might be related to the often observed existence, inside a gel, of microscopic heterogeneities at short length scales (generally of the order of 100 nm).^{26,27} Upon compression, the ‘voids’ in such heterogeneous textures would be expected to ‘shrink’ and/or somehow collapse, possibly beyond some critical compression. A convective expulsion of solvent would then result, leading to a weight loss of the sample, in qualitative agreement with the data in Fig.2. In terms of the macroscopic lateral expansion of the sample, the just mentioned mechanism would imply that the actual radius end up to be smaller than the one that would be obtained if the whole gel were incompressible. Again, this agrees with our observations in Fig.1. Looking at our data, we can then state that some water expulsion occurs in a range of compressions going from $\lambda \approx 0.94$ downwards while, at small deformations, the overall gel behaviour is in practice undistinguishable from that of an incompressible solid.

Let us now discuss force measurements in our compression experiments.

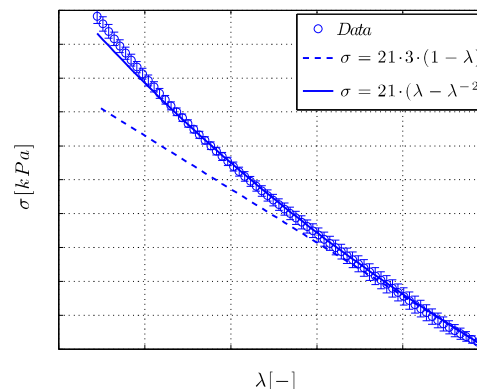


Figure 3. Variation of the nominal stress as function of the longitudinal compressive ratio. Data are averaged over twenty runs. Continuous line is the best fitting with a neo-Hookean incompressible equation, while dashed line is linear elasticity. From best fitting, the elastic modulus G is calculated, and it is $G = 21 \text{ kPa}$.

In Fig.3 we report the nominal stress ($\sigma \equiv f/\pi R_0^2$) as a function of the compressive ratio. We remind the reader that the data shown in Fig.3 are in fact averages taken over twenty compression ramps, at various strain rates, and that, since such data come out independent from the strain history, they can be taken as representative of the ‘instantaneous’ constitutive equation of the gel. For this reason, two theoretical predictions for the stress are also reported in Fig.3, namely, for a linear elastic solid and for a neo-Hookean solid, both of them supposedly incompressible. The data definitely show a linear

response of the stress vs. λ down to $\lambda \approx 0.9$ (say), and are quite well described by the neo-Hookean constitutive equation down to $\lambda \approx 0.8$, at least. In fact, the behaviour observed in Fig.3 is quite similar to what expected for an incompressible rubber. All of this agrees with rather common findings in the literature on physical gels, which perhaps justified the common credence that the linear regime in unconfined compression of gels holds up to 10-15% of strain.¹ On the other hand, our previous results here (in Figs.1, 2) do clearly indicate that incompressibility of the gel might not be a tenable assumption already for moderate strains. For our alginate gels, at least, we must be very cautious in gauging the linearity range from the data in Fig.3; even more suspicious is the seeming agreement between our data and the incompressible neo-Hookean constitutive equation. Actually, taken altogether, our results of Figs.1-3 make us deduce that the ‘instantaneous’ elasticity of our gel keeps linearity (and incompressibility) only down to $\lambda \approx 0.94$, i.e., up to 6% of compression. It is perfectly plausible that a similar warning is also valid for other physical gels.

A direct measurement of the shear stress τ_{xy} of the gel in a stress sweep (torsional) oscillatory experiment verified that the gel behaves as a linear elastic material, up to a shearing strain of $\gamma \approx 0.2$ at least, and hence well beyond 6%, as illustrated in Fig.4. Moreover, the value of the shear modulus obtained from the data in Fig.4 ($G = 22 \text{ kPa}$) quantitatively agrees with the ones (21 kPa) obtained from the fitting of the compression data in Fig.3 by either a neo-Hookean equation or a linear elasticity equation (at lower compressions).

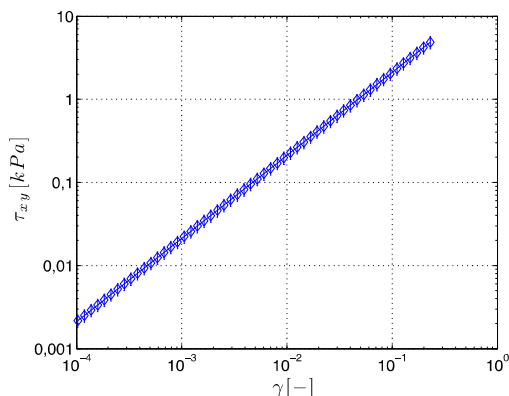


Figure 4. Stress sweep test at 1 Hz. Data are averaged over three runs.

Slope of the τ_{xy} vs γ in the double logarithmic scale is equal to 1, indicating a linear relationship between τ_{xy} and γ . Extrapolated intercept with $\gamma = 10^0$ gives a value of the modulus G of about 22 kPa , in nice agreement with the one estimated from compression tests (see Fig 3).

To summarize, the whole set of experiments reported here credibly testifies that, even in our case of a charged network (alginate chains plus water plus divalent cations), the dominant rheological contribution comes from the conformational entropy of the polymer chains, as in rubber elasticity. The conditions of incompressibility and linearity in the elastic behaviour are both found to hold for relatively small deformations only, i.e., up to 6% of compression.

Relaxation after compression

The previous analysis and conclusions have been further corroborated (and of course enriched) by stress-relaxation tests performed at various compression strains, on cylindrical samples

with identical diameters. The results, reported in terms of normalized force with respect to its initial value ($f(t)/f(0^+)$), are shown in Fig.5.

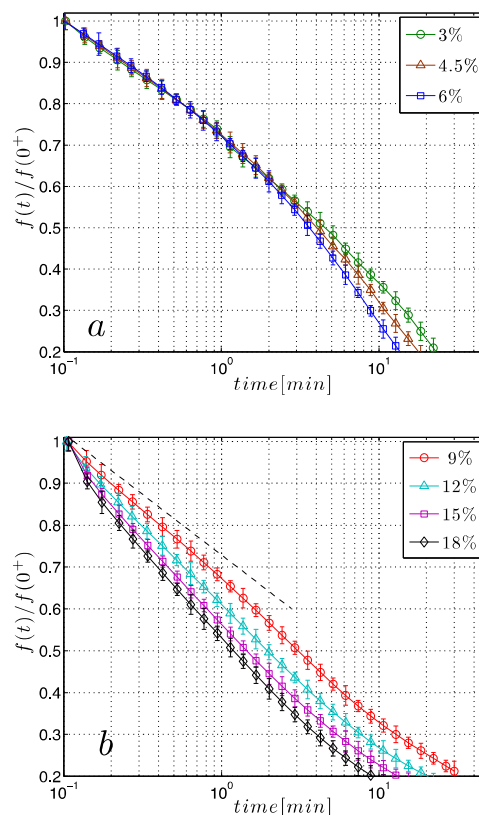


Figure 5. Normalized force relaxation curves upon compression, for different compressive strains ranging from 3 to 18%. Each set of data is averaged over three runs. Notice that, to avoid crowding of symbols, only some logarithmically equispaced data are shown. Above 6% of strain, a qualitative difference is observed between the two panels of data. The dashed line in panel *b* is the common early times slope of the relaxation curves in panel *a*.

The stress-relaxation curves up to 6% of compression (panel *a*) display a similar behaviour, while for higher values of strain (panel *b*) the curves increasingly deviate from each other, and are also qualitatively different from the relaxation curves at low strains. Here again, as from the experiments reported in the previous subsection, we envisage that the $\approx 6\%$ of compression is by some means a critical value, beyond which the gel behaviour changes, e.g., by the lack of incompressibility.

The low compression relaxation profiles are all found to exhibit the same trend in time, with distinct behaviours (on a semi-logarithmic scale) at short and long times. The early time decay is found to be the same for the three low compressions examined here, which is in fact the expected behaviour for a material within its linear viscoelasticity regime. (We remind the reader that the force measurements reported in Figs.5 are normalized with respect to the 0^+ force, i.e., the ‘instantaneous’ force upon compression.) On the other hand, the late time decays are different at different (but still low) compressions, indicating that, at ‘large’ times, some *compositional* and/or *structural* change is possibly taking place in the alginate gel. Thus, even when confining our experiments to compressions that have been judged

in the linear range of the ‘instantaneous’ elastic response of the incompressible gel (<6%, see previous subsection), a nonstandard relaxation sets in after a while, and, strictly speaking, a linear viscoelasticity range is no more identifiable.

As discussed to some extent in previous contributions by two of the present authors,^{28,21} the decay of force after application of a ‘small’ compression step to alginate gels can be ascribed to three diverse mechanisms: (i) constitutive (‘inner’) relaxation, most probably due to network rearrangements driven by combination and separation of ionic bonds among alginate chains; (ii) stress-diffusion coupling, related to the diffusion of water driven by a gradient in network stress, generated by the instantaneous compression; (iii) spontaneous (and usually slow) syneresis of the gel, maybe a consequence of some inherent meta-stability, unavoidably induced at the time of gel formation, and perhaps differently ‘activated’ at different compressions.

To investigate on the just mentioned different contributions to force relaxation, and to attempt to assess their timing for our alginate gels, we proceeded to perform unconfined compression experiments on cylindrical samples with different diameters, simultaneously monitoring the lateral surface of the gels, i.e., the sample radii, as a function of time. In Fig. 6, relaxation data of normalized force are reported, after a step compression with $\lambda = 0.97$, for three sample diameters $2R_0 = 15, 24, 35$ mm.

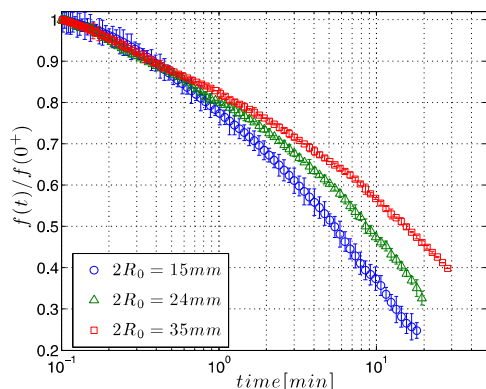


Figure 6 Normalized force relaxation behaviour vs. time for 3% compression at three sample radii (actual diameters are reported on the legend). Each data set is averaged over three runs. An effect of the sample radius is apparent at large times.

All data clearly show the two-decay relaxation already discussed above, when commenting Fig.5. Relaxations of samples with different radii are fairly similar up to around 1 min after the compression step, to depart from each other afterwards. It is apparent that, in the second decays, the force relaxes ‘faster’ as the initial radius is smaller. A ‘transition time’ around 1 min (say) from the compression step seems then to show in these data.

Let us now examine how the sample radii evolve in time. In Fig.7, the radial displacement $u_r(t) = r(t) - R_0$, normalized with its initial value $u_r(0^+) = r(0^+) - R_0$ right after the compression step, is reported as a function of time, again for three sample radii; in fact, the radii data in Fig.7 are obtained in the same experiments of the relaxation data in Fig.6.

Although less clearly than for the relaxation data, also the trend in time of the radius relaxation shows (on a semi-logarithmic scale) a ‘slow’ initial decay and a ‘faster’ subsequent one, and, again, a

time around 1-2 min after the compression step can be taken as a ‘transition time’. Also in the radii data, as for the force relaxation data, it can be seen that the smaller the initial radius, the steeper the relaxation.

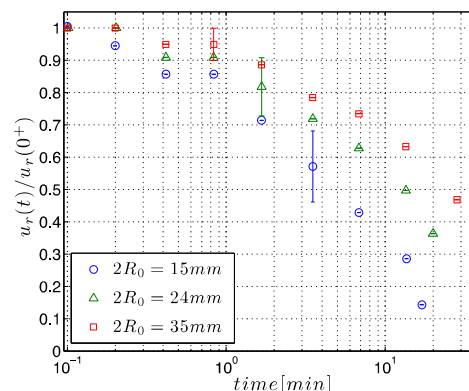


Figure 7 Normalized radial displacement as function of time for the three investigated radii. Radius measurements are obtained in the same experiments of fig. 6. For clarity, error bars are reported for some points only.

We are now in a position to discuss how the collected data can be interpreted in terms of the diverse mechanisms supposedly at work in the relaxing gel. The key observation to be made concerns the ‘early times’ reduction of the gel radius, up to around 2 min. Within such a time span, the radial displacement $u_r(t)$ is found to decrease by ca. 20%-30% with respect to its initial value. Since a radius decrease must always go together with water transport outwards the gel, and since syneresis does not typically affect materials’ behaviour at early times, we must conclude that, already within a time span soon after the deformation, a stress-diffusion coupling mechanism is active. The question is: is stress-diffusion coupling the only active mechanism during early relaxation? In other words, is there any indication of a co-occurrence of diverse relaxation mechanisms? Our answer to the latter question will be given on a twofold basis. First, we re-plot the force relaxation data of Fig.6 in terms of a rescaled time, namely, the ratio of actual time to the sample radius R_0 before compression (radius after conditioning).

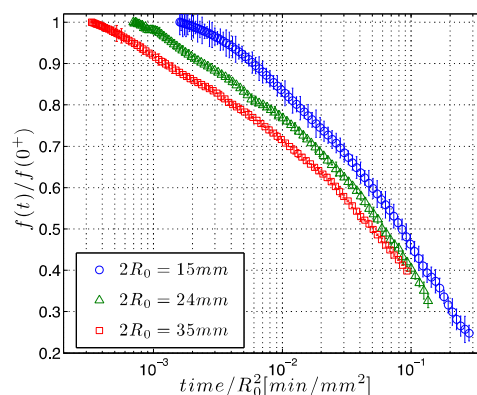


Figure 8 Same force relaxation data of Fig. 6 vs. the re-scaled time (t/R_0^2). Rescaled data do not collapse on a single curve or portion of curve, indicating that solvent diffusion is not the only active relaxation mechanism after the compression step.

With such a rescaling, usual for a diffusion-driven process, one

should find data from samples at different radii collapsing on a single curve, if diffusion were the only driving force. This is clearly not the case for our data, as seen in Fig.8: data pertaining to different sample radii stay well distinct. Curiously enough, a

5 tendency to a common trend can instead be found at large times. As a second step in our analysis, we make use of the Doi's theory of linear stress-diffusion coupling to calculate the drop in force due to diffusive mechanism from the knowledge of the gel radius during relaxation, see Fig.7. Indeed, the normalized force decay

10 is calculated from Doi's theory as: ⁵

$$\frac{f(t)}{f_0} = \frac{2}{3} \left[1 - \frac{u_r(t)}{R_0} \frac{1}{(1-\lambda)} \right] \quad (2)$$

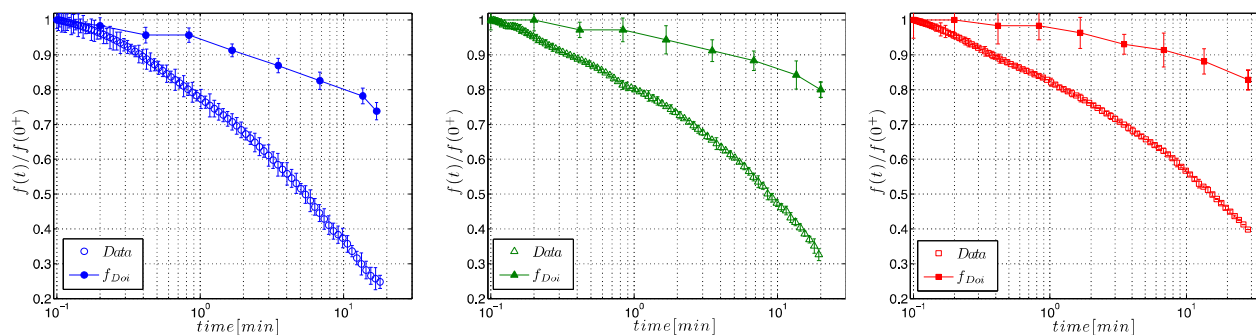


Figure 9 Normalized force vs. time upon 3% compression for the three different diameters investigated, 15, 24, and 35 mm from left to right. Filled symbols are normalized force predictions based on Doi equation (eq. 2), where the only active mechanism of relaxation is water diffusion. The measured relaxation is undoubtedly faster than predicted.

From the above results, we can definitely conclude that the observed force relaxation and water expulsion up to the 'transition time' cannot be ascribed to stress-diffusion coupling only. In the next subsection, therefore, the existence and possible relevance of an intrinsic relaxation mechanism will be discussed in some detail.

Relaxation after torsion, and storage and loss moduli

In figures 10 and 11, the relaxation behaviour of the gel after a step torsional deformation is shown, in terms of measured torque M and normal force f_N , respectively. In both figures, data are reported on cylindrical samples with three different diameters. As mentioned in the Materials & Methods section, the plates of the rheometer are now treated so that a no-slip condition between the gel and the wall hold. We signal to the reader that torque relaxation experiments at different 'low' strains (i.e. $\gamma = 0.01, 0.03$, and 0.06) gave exactly superimposable normalized results (data not shown), as expected in the linear viscoelasticity range; as a consequence, no variation of the gel radius should show in these deformations, as we indeed confirmed in our experiments (for not too large times, at least).

For around two decades in time, hence again up to around 2 min after the step deformation, torque in Fig.10 essentially displays the same behaviour for the three investigated radii, namely, a logarithmic decay, whereas slight (but reproducible) differences become visible afterwards. (The line in Fig.10 is the result of a model to be discussed below.) The appearance once more here of a 'transition time', comparable to the one found in compression experiments, is further (and strongly) confirmed by the normal

where $(1 - \lambda)$ is the applied strain (3% in all our compressive tests). Thus, from the available experimental data of the radii vs. time of Fig.7, we can obtain the corresponding forces as predicted through Eq.2, to be compared with the measured ones. Fig.9 shows both Doi's calculation and the experiments. It is apparent that the calculated force relaxations stay well higher than the measured ones. Again considering the situation at $t = 2 \text{ min}$ (i.e., at the 'transition time'), we find that Doi's normalized force is around 0.9, whereas measured values are in between 0.7-0.75: such discrepancy is well outside experimental uncertainties.

55 force data reported in Fig.11.

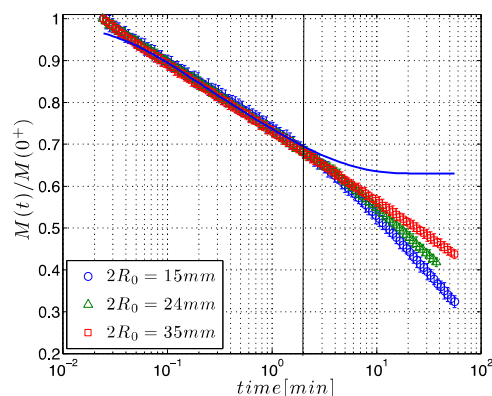


Figure 10 Normalized torque relaxation curves after a step torsion of 3% at different sample radii. Each data set is averaged over three runs. Collapse is observed up to a characteristic time of 2 min (the 'transition time' discussed in the text), indicated here with a vertical bar. The continuous curve in the plot is a best fitting from the model described in the appendix of the paper, accounting for network relaxation. The model is so conceived as to work properly only up the transition time.

In principle, for torsional linear deformations, no normal force should arise at all and, indeed, this expectation is fulfilled by our data up to 2 min after the torsion. At larger times, conversely, a normal force grows, the more so the smaller the sample radius. This unexpected behaviour might perhaps be linked to a structural 'slow' change in the gel (the above mentioned mechanism (iii)), the discussion of which, however, is far beyond the purpose of the present paper. We simply signal here how the

late appearance of a normal force in the relaxation after a torsion connotes a nonstandard viscoelasticity for our gels.

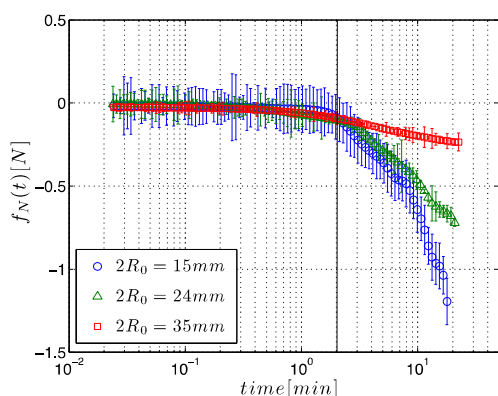


Figure 11 Normal force as function of time measured in the torsional experiments of Fig.10. Here, as in the previous figure, the vertical bar marks a ‘transition time’. Notice the growth of normal force beyond the transition time, for all the investigated radii.

On the other hand, the experimental results in Figs 10, 11 in the first two time decades, i.e., up to 2 min after a torsion, can be seen as representative of a standard linear viscoelasticity of the gel. To further emphasize this feature, we performed a frequency sweep test on the gel, to obtain its storage and loss modulus as function of frequency, in the range of frequencies corresponding to the just mentioned two decades in time. The obtained data, shown in Fig.12, are indeed as expected for a gel, with a (weakly increasing) elastic modulus much higher than the loss modulus throughout two frequency decades.

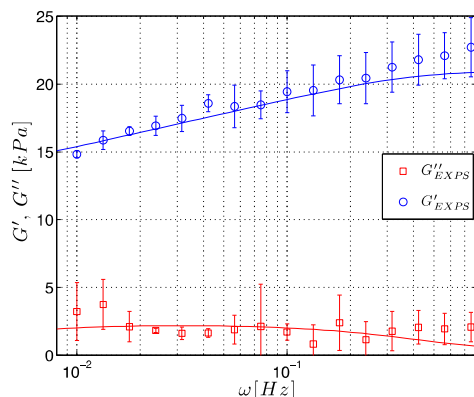


Figure 12. Symbols: averaged results over three frequency sweep tests at 1% torsional strain, for a cylindrical sample of 35 mm diameter. Lines: calculated $G'(\omega)$ and $G''(\omega)$ from the model reported in the appendix of the paper, with the same parameters used to obtain the $G(t)$ curve of Fig.10. Notice that the range of frequency reported in the figure corresponds to the range of time up to the transition time $t = 2 \text{ min}$ (see text).

To complete the picture, we also report in Fig.12 the calculated storage and loss moduli as function of frequency, as predicted from the model described in the appendix of the paper. For the sake of clarity, we proceeded by first fitting the relaxation data of Fig.10 with such a model, thus obtaining the relaxation spectrum, to eventually compute the moduli. All the details of this procedure and the numerical values of the parameters are reported in the Appendix.

The nice agreement between the observed and calculated moduli shown in Fig.12 confirms that torsional relaxation experiments are well understood in the frame of standard linear viscoelasticity up to the ‘transition time’, $t = 2 \text{ min}$. The torque relaxation data in Fig.10, up to 2 min after the torsion step, are the clear signature of a constitutive (‘inner’) relaxation of the network component of the gel, which we mentioned previously (mechanism (i)).

An interpretation of the gel relaxation behaviour

Putting together all the information from the previous two subsections, we envisage that the above mentioned mechanisms of constitutive relaxation and stress-diffusion coupling are most probably co-occurring in the alginate gel, after a compression step, for a certain time span, i.e., up to the transition time. In the long-time response of the material, on the other hand, a complex additional gel rearrangement takes place, with peculiar features.

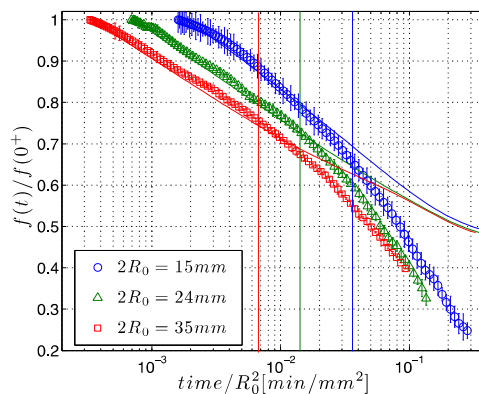
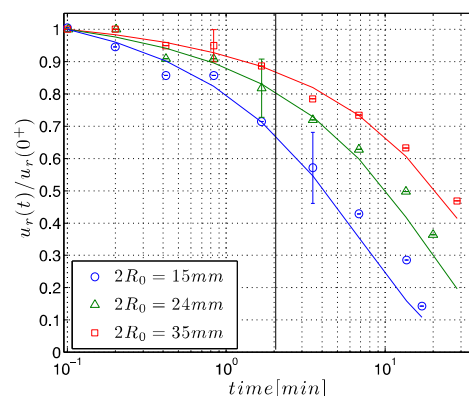


Figure 13 Same data of Figs 7 and 8 along with model simulation. The model, described in the appendix, is expected to work properly only up to the transition time $t = 2 \text{ min}$ (see text). Notice that, in the bottom panel, the rescaled transition times are indicated by vertical bars corresponding to different radii.

Limiting ourselves to the short-time gel response, we have already shown (see Fig.9) how Doi’s theory of stress-diffusion coupling, in its original version, is not capable of predicting the results of our relaxation experiments. In this section, we will illustrate how instead a simple extension of Doi’s theory, recently proposed by two of the present authors,²⁸ comes out in reasonable agreement with the relaxation data.

In our novel model, the gel is regarded as a homogeneous mixture of a solvent and a viscoelastic solid. In the present case, such viscoelastic solid is the physical network of the alginate. The

mechanical relaxation of the gel is then due to both solvent transport in/out of the gel and constitutive relaxation of the network. The model is sketchily described in the Appendix, where the adopted equations and the evaluation of the model parameters are also reported. In Fig. 13, we report the model predictions together with the experimental data of Figs 7 and 8: it can be seen that agreement is pretty good. In this respect, we would like to emphasize that such agreement with six data sets is obtained through only two adjustable parameters (namely, a Darcy constant κ , and a Lamè constant λ_M , see appendix). As expected, the fitting quality degrades as we approach the transition time, where syneresis starts to prevail. From the agreement among data and predictions up to the transition time, however, we can conclude that both mechanisms of inner relaxation and stress-diffusion coupling are at play, and that the proposed model correctly describes such interplay.

Conclusions

In the present work, we performed an analysis of the different relaxation mechanisms active in an alginate-based ionic gel. Several mechanical tests were carried out: compressive stress-strain measurements at different strain rates, to evaluate the range of ‘instantaneous’ linear elasticity; stress relaxation at different compressions, to evaluate the range of linear visco-elasticity; stress-relaxation upon compression on samples with different diameters, to assess the different relaxation mechanisms of the gel; stress relaxation upon torsional deformations, to study relaxation behaviour without solvent transport. In most cases we measured, with the aid of a CCD camera, the changes in the radius of the sample during test.

The obtained results can be summarized in the following points.

i) By ‘instantaneous’ deformations, the gel, as a whole, responds as a linear incompressible elastic material only up to 6% of strain. Compressive and torsional data agree (within experimental error) to identify such upper limit. Beyond 6% in strain, the gel is compressible, as it is clearly evidenced from the comparison of the actual radius vs. the theoretical one (i.e., for an incompressible material), and from the variations of weight loss after compressions. The measurements show that the compressibility of the gels results in water expulsion. Such expulsion, maybe through some convective mechanism, conceivably is a direct consequence of the heterogeneity of the gel on a mesoscopic length scale. The whole range of results of the stress-strain test in compression closely follows a neo-Hookean behaviour.

ii) The stress relaxation tests also show a linear range up to about 6%, consistent with the data of ‘instantaneous’ stress. Both torsion and compression display a double relaxation regime, with a ‘transition’ at about 2 minutes from the imposed deformation step. Measurement of the normal force after a torsion step clearly shows that syneresis effects dominate the relaxation at times larger than 2 min.

iii) For times less than 2 minutes, it is necessary to distinguish between torsional and compressive tests. From the measurements of relaxation in torsion, where the effect of stress-diffusion coupling is confirmed to be nil, it is possible to evaluate the contribution of the relaxation caused by inner rearrangements of the network. The inner relaxation mechanism follows a

logarithmic decay in time; relaxation can then be described through a distribution of characteristic times. On the other hand, compression tests at different radii show that the force decay is not attributable solely to water diffusion. In this case, both mechanisms of inner relaxation and diffusion are active.

Finally, we applied a generalized *two-fluid model*, recently developed by two of the present authors, to simulate the relaxation tests in compressions with different sample radii. To describe the network relaxation, we used a generalized Maxwell model, with 4 viscoelastic characteristic times and a steady-state linear elastic response (see appendix). Most model parameters were evaluated through a best fitting procedure of the relaxational data in torsion. Thereafter, fitting of the data in compression was worked out with a reduced number (2) of adjustable parameters. The model is capable to quite reasonably describe the coupling between the internal relaxation and diffusion, and the available data, up to the advent of syneresis.

Appendix

The *fluid-viscoelastic solid* model recently proposed by two of the present authors is here briefly summarized. The restricted version of such model that is adopted to describe our alginate-based gel is also described here, and the values of the model parameters needed for data fitting are given.

The model belongs to a general category of models termed as ‘non-classical mixture theory’,⁵ where the overall response of a mixture is described in terms of fields somehow peculiarly attributed to one or the other of the ‘components’ of the mixture.

In our case of a gel, the two components are the solvent fluid and the polymer network solid. Under various simplifying assumptions, discussed in detail elsewhere²⁸, the model equations are:

$$\nabla \cdot \frac{\partial \mathbf{u}^{(N)}}{\partial t} = \kappa \nabla^2 p^{(S)} \quad (\text{A1})$$

$$\nabla \cdot (\mathbf{T}^{(N)} - p^{(S)} \mathbf{I}) = \mathbf{0} \quad (\text{A2})$$

where, as mentioned above, a pressure $p^{(S)}$ is attributed to the solvent, a velocity $\partial \mathbf{u}^{(N)} / \partial t$ is attributed to the network (the field $\mathbf{u}^{(N)}(\mathbf{r}, t)$ is the displacement at time t of a network point that was at \mathbf{r} in a reference state), and $\mathbf{T}^{(N)}$ is the network stress tensor. Equation (A1) is a Darcy-like equation, describing solvent permeation through the network ‘matrix’, with κ the solvent/network permeability constant. Equation (A2) is the momentum balance equation for the overall gel, made up of solvent and network. Notice that inertia was neglected in eq. (A2).

To solve for solvent pressure and network velocity (hence, for network displacement), Equations (A1) and (A2) must be closed by a constitutive equation for the network stress $\mathbf{T}^{(N)}$. In ref. 28, the case was discussed where the network stress is that of a linear viscoelastic solid, with a single relaxation time τ . The generalization to multiple relaxation times is straightforward: the linear viscoelastic solid is described through a multimode scheme, and the network stress is the sum of the stresses $\{\mathbf{t}_i\}$ from each of the modes:

$$\tau_i \frac{\partial \mathbf{t}_i}{\partial t} + \mathbf{t}_i = 2G_{\infty,i} \mathbf{E}^{(N)} + 2G_{0,i} \tau_i \mathbf{D}^{(N)} + 2[\lambda_{\infty,i} \text{tr}(\mathbf{E}^{(N)}) + \lambda_{0,i} \tau_i \text{tr}(\mathbf{D}^{(N)})] \mathbf{I} \quad (\text{A3})$$

$$\mathbf{T}^{(N)} = \sum_i \mathbf{t}_i \quad (\text{A4})$$

In such constitutive equations, $\mathbf{E}^{(N)} = 1/2(\nabla \mathbf{u}^{(N)} + (\nabla \mathbf{u}^{(N)})^T)$ is the symmetrized deformation tensor from the network displacement $\mathbf{u}^{(N)}(\mathbf{r}, t)$, $\mathbf{D}^{(N)} = \partial \mathbf{E}^{(N)} / \partial t$ is the rate-of-deformation tensor, and $\text{tr}(\cdot)$ is the trace operator. The constants $G_{\infty,i}$, $G_{0,i}$ are shear moduli, $\lambda_{\infty,i}$, $\lambda_{0,i}$ are Lamè constants, and τ_i is the characteristic time of the i -th mode of the network.

Equation (A3) above give the most general form for the i -th ('partial') stress for a linear viscoelastic solid. In dealing with our alginate-based ionic gel, we decided to adopt a *minimal version* of such equations, so as to minimize the number of parameters, and found that the following set of equations is, in fact, fully appropriate:

$$\tau_i \frac{\partial \mathbf{t}_i}{\partial t} + \mathbf{t}_i = 2G_M \tau_i \mathbf{D}^{(N)} + 2\lambda_M \tau_i \text{tr}(\mathbf{D}^{(N)}) \mathbf{I}, \quad i = 1, \dots, 4 \quad (\text{A3}')$$

$$\mathbf{t}_5 = 2G_{\infty} \mathbf{E}^{(N)}$$

Indeed, the measured gel relaxation after a torsion step (and up to the 'transition time') can be well described by the above Eqs. A3', A4, as illustrated in Fig.10 in the main text. The needed parameter values, obtained through a fitting procedure of the torsion step relaxation data, are reported in Table 1. We recall that the analysis was restricted to the first 2 min of relaxation. Beyond such time, we assumed that no further inner relaxation occur: the network response at long times is that of an ideal elastic solid, with modulus equal to G_{∞} .

Table 1 Model parameters from best fitting of data of relaxation in torsion (fig. 10). The reported moduli are normalized with respect to the shear modulus $G = 21 \text{ kPa}$

τ_1 [min]	τ_2 [min]	τ_3 [min]	τ_4 [min]	$\bar{G}_M[-]$	$\bar{G}_{\infty}[-]$
0.0794	0.2818	1.0	3.548	0.0925	0.63

With those same parameters, the frequency response is readily calculated through the following analytic expressions:

$$G'(\omega) = G_{\infty} + G_M \sum_{i=1}^4 \frac{\tau_i^2 \omega^2}{1 + \tau_i^2 \omega^2} \quad (\text{A5})$$

$$G''(\omega) = G_M \sum_{i=1}^4 \frac{\tau_i \omega}{1 + \tau_i^2 \omega^2}$$

and the agreement with the corresponding data is shown in Fig.12 in the main text.

The possible co-occurrence of constitutive relaxation with solvent diffusion is also covered by the complete model, i.e., with all Eqs. A1, A2, A3', and A4. Indeed, the complete mathematics of the

relaxation after a step uniaxial compression of a laterally unconfined cylindrical sample gives the predictions shown in Fig.13 of the main text. Having already fixed six of the parameters on the basis of the torsional response of the gel (see Table 1), the remaining two parameters are the Lamè constant (λ_M) and the Darcy constant (κ). These two parameters were indeed determined through a best fitting procedure involving all compression data for the three examined radii, i.e., the three normalized relaxation forces, and the corresponding three changes in the normalized radius. The parameter values of the best-fitting procedure are: $\lambda_M = 1526 \text{ Pa}$ and $\kappa = 0.9 \cdot 10^{-4} \text{ mm}^2 / \text{Pa min}$.

Acknowledgment

Ministero dell'Istruzione dell'Università e della Ricerca MIUR (project PRIN 2010–2011 Prot. 20109PLMH2_005) is gratefully acknowledged. We would also thank Mrs A. Aldi for helping in the preparation of the gel.

Notes and references

- ^a Institute of Polymer Composite and Biomaterials – National Research Council of Italy,– P.le E. Fermi 1, 80055 Portici, Naples, Italy, and INSTM UdR of Naples, Italy. Fax: +39 081 7758850; Tel: +39 081 7758810; E-mail: larobina@unina.it
- ^b Institute for Research on Combustion – National Research Council of Italy,– P.le V. Tecchio 80, 80125 Naples, Italy. Fax: +39 081 5936936; Tel: +39 081 7682275; E-mail: fgreco@irc.cnr.it
- 1 X. Zhao, N. Huebsch, D. J. Mooney, and Z. Suo, *Journal of applied physics*, 2010, **107**(6), 063509.
- 2 C. Tsitsilianis, and I. Iliopoulos, *Macromolecules*, 2002, **35**(9), 3662–3667.
- 3 E. Geissler, and A. M. Hecht, *Macromolecules*, 1980, **13**(5), 1276–1280.
- 4 E. Geissler, and A. M. Hecht, *Macromolecules*, 1981, **14**(1), 185–188.
- 5 T. Yamaue, and M. Doi, *The Journal of chemical physics*, 2005, **122**(8), 084703.
- 6 Z. I. Kalcioğlu, R. Mahmoodian, Y. Hu, Z. Suo, and K. J. Van Vliet, *Soft Matter*, 2012, **8**(12), 3393–3398.
- 7 G. W. Scherer, *Journal of Non-Crystalline Solids*, 1988, **100**(1), 77–92.
- 8 S. Boral, A. Saxena, and H. B. Bohidar, *International journal of biological macromolecules*, 2010, **46**(2), 232–236.
- 9 W. Pilnik, and F. M. Rombouts, *Carbohydrate research*, 1985, **142**(1), 93–105.
- 10 O. Smidsrød, and G. Skja, *Trends in biotechnology*, 1990, **8**, 71–78.
- 11 E. Alsberg, K. W. Anderson, A. Albeiruti, R. T. Franceschi, and D. J. Mooney, *Journal of dental research*, 2001, **80**(11), 2025–2029.
- 12 K. I. Draget, O. Smidsrød, and G. Skjåk-Braek, *Polysaccharides and Polyamides in food industry*, 2005, **1**, 143.
- 13 G. T. Grant, E. R. Morris, D. A. Rees, P. J. Smith, and D. Thom, *FEBS letters*, 1973, **32**(1), 195–198.
- 14 H. J. Kong, D. Kaigler, K. Kim, and D. J. Mooney, *Biomacromolecules*, 2004, **5**(5), 1720–1727.
- 15 M. Mancini, M. Moresi, and R. Rancini, *Journal of Food Engineering*, 1999, **39**(4), 369–378.
- 16 M. Moresi, M. Mancini, M. Bruno, and R. Rancini, *Journal of texture studies*, 2001, **32**(5□6), 375–396.
- 17 M. Papageorgiou, S. Kasapis, and M. G. Gothard, *Carbohydrate polymers*, 1994, **24**(3), 199–207.
- 18 M. Moresi, M. Bruno, and E. Parente, *Journal of food engineering*, 2004, **64**(2), 179–186.
- 19 J. R. Mitchell, *Journal of Texture Studies*, 1976, **7**(3), 313–339.
- 20 A. Nussinovitch, M. Peleg, and M. D. Normand, *Journal of Food Science*, 1989, **54**(4), 1013–1016.
- 21 G. Gentile, F. Greco, and D. Larobina, *European Polymer Journal*, 2013, **49**(12), 3929–3936.

-
- 22 D. Larobina, and L. Cipelletti, *Soft Matter*, 2013, **9**(42), 10005-10015.
- 23 M. A. LeRoux, F. Guilak, and L. A. Setton, *Journal of biomedical materials research*, 1999, **47**(1), 46-53.
- 24 R. E. Webber, and K. R. Shull, *Macromolecules*, 2004, **37**(16), 6153-
5 6160.
- 25 K. I. Draget, K. Østgaard, and O. Smidsrød, *Carbohydrate Polymers*,
1990, **14**(2), 159-178.
- 26 A. M. Hecht, R. Duplessix, and E. Geissler, *Macromolecules*, 1985,
18(11), 2167-2173.
- 10 27 R. Liu, and W. Oppermann, *Macromolecules*, 2006, **39**(12), 4159-
4167.
- 28 D. Larobina, and F. Greco, *The Journal of chemical physics*, 2012,
136(13), 134904.

We investigated the presence of different contributions to force relaxation in ionically cross-linked alginate gels, and attempted to assess their timing.

